Effects of Self-Complementarity, Codon Optimization, Transgene, and Dose on Liver Transduction with AAV8

Peter Bell, Lili Wang, Shu-Jen Chen, Hongwei Yu, Yanqing Zhu, Mohamad Nayal, Zhenning He, John White, Deborah Lebel-Hagan, and James M. Wilson*

Gene Therapy Program, Department of Medicine, Perelman School of Medicine, University of Pennsylvania, Philadelphia, Pennsylvania.

Numerous methods of vector design and delivery have been employed in an attempt to increase transgene expression following AAV-based gene therapy. Here, a gene transfer study was conducted in mice to compare the effects of vector self-complementarity (double- or single-stranded DNA), codon optimization of the transgene, and vector dose on transgene expression levels in the liver. Two different reporter genes were used: human ornithine transcarbamylase (*hOTC*) detected by immunofluorescence, and enhanced green fluorescent protein (*EGFP*) detected by direct fluorescence. The AAV8 capsid was chosen for all experiments due to its strong liver tropism. While *EGFP* is already a codon-optimized version of the original gene, both wild-type (WT) and codon-optimized (co) versions of the *hOTC* transgene were compared in this study. In addition, the study evaluated which of the two *hOTC* modifications—codon optimization or self-complementarity—would confer the highest increase in expression levels at a given dose. Interestingly, based on morphometric image analysis, it was observed that the difference in detectable expression levels between self-complementary (sc) and single-stranded (ss) *hOTC*co vectors was dose dependent, with a sevenfold increase in OTC-positive area using sc vectors at a dose of 3×10^9 genome copies (GC) per mouse, but no significant difference at a dose of 1×10^{10} GC/mouse. In contrast, with *EGFP* as a transgene, the increases in expression levels when using the sc vector were observed at both the 3×10^9 GC/mouse and 1×10^{10} GC/mouse doses. Furthermore, codon optimization of the *hOTC* transgene generated a more significant improvement in expression than the use of self-complementarity did. Overall, the results demonstrate that increases in expression levels gained by using sc vectors instead of ss vectors can vary between different transgenes, and that codon optimization of the transgene can have an even more powerful effect on the resulting expression levels.

Keywords: AAV8, liver gene transfer, self-complementarity, codon optimization

INTRODUCTION

AAV VECTORS HAVE BEEN modified in a variety of ways to increase expression of the encoded transgene. A limiting factor in efficiency of transgene expression not determined by the capsid is the formation of double-stranded vector genomes within the host cell.[1,2] After entry into the cell nucleus, the single-stranded (ss) AAV DNA undergoes replication using the host cell DNA polymerase, resulting in a double-stranded AAV genome that is then able to begin transcription of the transgene (reviewed in McCarty[3]). Alternatively, double-stranded genomes also appear to be formed by the joining of complementary ss genomes that may be present within the same cell.[4] To circumvent the rate-limiting step of duplex DNA formation within the cell, self-complementary (sc) versions of AAV vectors have been engineered. This can be achieved by producing vectors where Rep endonuclease is unable to nick the terminal resolution site due to its deletion, re-

*Correspondence: Dr. James M. Wilson, Gene Therapy Program, Department of Medicine, University of Pennsylvania, 125 S. 31st Street, TRL 2000, Philadelphia, PA 19104. E-mail: wilsonjm@upenn.edu

DOI: 10.1089/hgtb.2016.039

sulting in the newly replicated strand remaining bound to the template strand.[5,6] Numerous studies have shown that such sc vectors can achieve higher transgene expression levels than their ss counterparts.[3] However, it has also been noted that the titers of sc vectors established through quantitative PCR (qPCR) can have a lower readout due to rapid self-annealing of the complementary strands, thereby inhibiting the binding of primers.[7] Caution must therefore be taken in the quantification of sc vectors by PCR methods in order to avoid underreporting of titers and therefore overdosing of animals. A further drawback of sc vectors is their decreased capacity in transgene size, which is typically half the length of the ss genome, making their use challenging for large transgenes.

A variety of other modifications of the transgene cassette can be employed to increase expression, such as the use of cis-regulatory elements or adjustment of the CG content. One particularly successful strategy to enhance expression is to codon optimize the sequence of the transgene, which involves the use of codons specific for a given host organism that allow optimal protein synthesis during translation without changing the amino acid sequence.[8–10] Codon optimization has been particularly appealing when expressing secreted proteins, such as coagulation factors, since relatively small numbers of transduced cells could theoretically be sufficient to secrete therapeutic levels of protein.[11–14] In fact, codon-optimized vectors expressing the secreted human enzyme α-L-iduronidase (hIDUA) were successfully applied to dog and cat models of mucopolysaccharidosis type I (MPS I). When administered systemically early after birth, expression levels were sufficient to induce tolerance against the human protein in MPS I dogs.[15–17] Correction of brain pathology was also achieved in this model, with high expression levels of the secreted protein likely allowing cross-correction of untransduced cells. Enhanced expression of another codon-optimized transgene, factor VIII, in the liver has also been shown to induce tolerance in mice that is capable of avoiding inhibitor formation.[18] Codon optimization of AAV-encoded transgenes has also been used to increase the expression of non-secreted proteins in mice, such as dystrophin,[19] survival of motor neurons,[20] and ornithine transcarbamylase (OTC).[21] Long-term safety and efficacy of factor IX (FIX) gene therapy has been demonstrated in hemophilia B patients treated with an sc AAV8 vector encoding codon-optimized human *FIX*.[22,23]

While numerous reports have investigated the ability of self-complementarity or codon optimization to improve levels of AAV-mediated transgene expression in animal models, few reports have documented a direct comparison between these two vector modifications while also taking into account the potentially confounding impact of transgene and dose. This study attempts to determine the cumulative impact of these factors on transgene expression levels in the mouse liver following AAV8-based gene transfer. The findings indicate that the improved expression gained by sc vectors, as opposed to ss vectors, can be both transgene- and dose-dependent. In addition, compared with the conversion from ss to sc, the process of codon optimization yields an even greater improvement in the levels of transgene expression achieved.

MATERIALS AND METHODS

AAV vectors and production

AAV8 expressing either human OTC (hOTC) or enhanced green fluorescent protein (EGFP) from the liver-specific thyroxine-binding globulin (TBG) promoter[24] was utilized as the general vector platform. The *EGFP* gene is identical to the sequence in pEGFP-C1 (Clontech). The following individual vectors were injected into mice: ss AAV8 encoding co hOTC and carrying the woodchuck hepatitis virus posttranscriptional regulatory element (WPRE; AAV8ss.TBG.hOTCco.WPRE), sc AAV8 encoding wild-type (non-codon-optimized) hOTC (AAV2/8sc .TBG.hOTC-WT), sc AAV8 encoding co hOTC (AAV8sc.TBG.hOTCco), ss AAV8 encoding EGFP and carrying the WPRE (AAV8ss.TBG.EGFP.WPRE), and sc AAV8 encoding EGFP (AAV8sc.TBG.EGFP).

AAV vectors were produced by the Penn Vector Core at the University of Pennsylvania, as previously described.[25] Vector preps were titered by qPCR targeting the poly-A region of the expression cassette and dosing of animals was based on this titer. To address potential variabilities of these assays, additional titrations were performed with qPCR targeting the TBG promoter region, yielding similar results with <1.4-fold differences (data not shown). As a third method, droplet digital PCR (ddPCR) was performed, as previously described.[26] This more sensitive method yielded consistently higher titers ranging from 1.8-fold to 4.4-fold higher values compared with the pA qPCR titers (data not shown).

Codon optimization of the *hOTC* sequence to adjust for optimal expression in human cells was performed by GenScript (Piscataway, NJ) using their proprietary OptimumGene™ codon-optimization technology, and the DNA sequence was further modified to eliminate potential alternative reading frames from internal out-of-

frame ATGs with a size equal to or greater than nine peptides, as described previously.[21]

Animals

All experiments were performed in male spf^{ash} mice bred in the laboratory. This mouse strain expresses only low levels of endogenous OTC not detected by immunostaining.[21,27] All mice were maintained at the Animal Facility at the University of Pennsylvania under protocols reviewed and approved by the University of Pennsylvania's Institutional Animal Care and Use Committee. All experiments performed in animals followed institutional guidelines and regulations. The vectors were administered by tail-vein injection at two doses: 3×10^9 or 1×10^{10} genome copies (GC)/animal ($n=5$). Animals were necropsied at days 14 or 15, and the livers were processed for histology and vector genome analysis. Spf^{ash} mice that did not receive the vectors served as controls.

Histology

For detection of EGFP, livers were fixed overnight in 10% neutral buffered formalin (Fisher), washed in phosphate-buffered saline, embedded in OCT compound (VWR), and flash-frozen for cryosectioning. Frozen sections at a thickness of 8 μm were prepared and mounted with Vectashield mounting medium (Vector Laboratories). To detect hOTC expression, livers were frozen without prior fixation, and cryosections at 8 μm were processed for immunofluorescence staining as described[27] using a rabbit polyclonal antibody raised against OTC (provided by Hiroki Morizono, Children's National Medical Center, Washington, DC) and a FITC-labeled secondary antibody (Jackson Immuno Research Laboratories).

Determination of vector genomes in the liver

Vector GCs in the liver were analyzed by real-time PCR (TaqMan UniversalMasterMix, Applied Biosystems), as described previously.[28]

Image analysis

To quantify both EGFP and hOTC expression in the liver, 10 random images were taken from each section with a 10× objective on a Nikon Eclipse Ti-E microscope under identical settings for each transgene. The images were analyzed for the percentage of transgene-positive area and for the intensity of GFP or OTC immunostain fluorescence. One animal from group 7 showed no expression, likely due to failed injection, and was excluded from the analysis.

For area analysis, images were thresholded (*i.e.*, GFP- or OTC-positive liver areas were selected) using ImageJ software (Rasband W.S., National Institutes of Health; http://rsb.info.nih.gov/ij/). To establish background values for both GFP fluorescence and OTC immunofluorescence and to be able to distinguish with confidence between positive and negative liver areas, sections from untreated control mice were included into the thresholding process and morphometric analysis. The percentage of GFP- or OTC-positive image area was then determined with the ImageJ program using the images from the control animals as baseline for negative liver area. To correct for "empty" areas such as veins and sinusoids, the percentage of such areas was first determined for each image by thresholding with ImageJ and then subtracted from the total area to calculate the percentage of transgene-positive hepatocytes. No other cell types appeared to be transduced.

To measure fluorescence intensity, 10 liver images from each animal were analyzed with ImageJ to determine the mean pixel intensity (*i.e.*, the mean gray value) for each image.

Statistical analysis

One-way analysis of variance followed by Tukey's test was performed to compare the means of groups using GraphPad Prism v6.03 (GraphPad Software).

Protein quantification

EGFP in the liver was quantified using an enzyme-linked immunosorbent assay (ELISA), as previously described.[29] OTC protein was quantified on Western blots. Approximately 5 μg of total protein from mouse liver lysates were separated using a 4–20% Tris glycine polyacrylamide gel. Membranes with transferred protein bands were probed with a mouse monoclonal antibody against OTC (Abcam) and a rabbit monoclonal antibody against cyclophilin A as reference protein. Bound primary antibodies were detected with IRDye® 800CW goat anti-mouse IgG (H + L) and IRDye 700CW donkey anti-rabbit IgG (H + L; Licor) using a Licor Odyssey CLx instrument. OTC expression was then normalized to cyclophilin A using the image studio program (Licor).

RESULTS AND DISCUSSION

In these studies, AAV8 vectors were used expressing one of two transgenes (*hOTC* or *EGFP*) with two dosing groups (3×10^9 or 1×10^{10} GC/mouse, $n=5$), and tissue was harvested 2 weeks

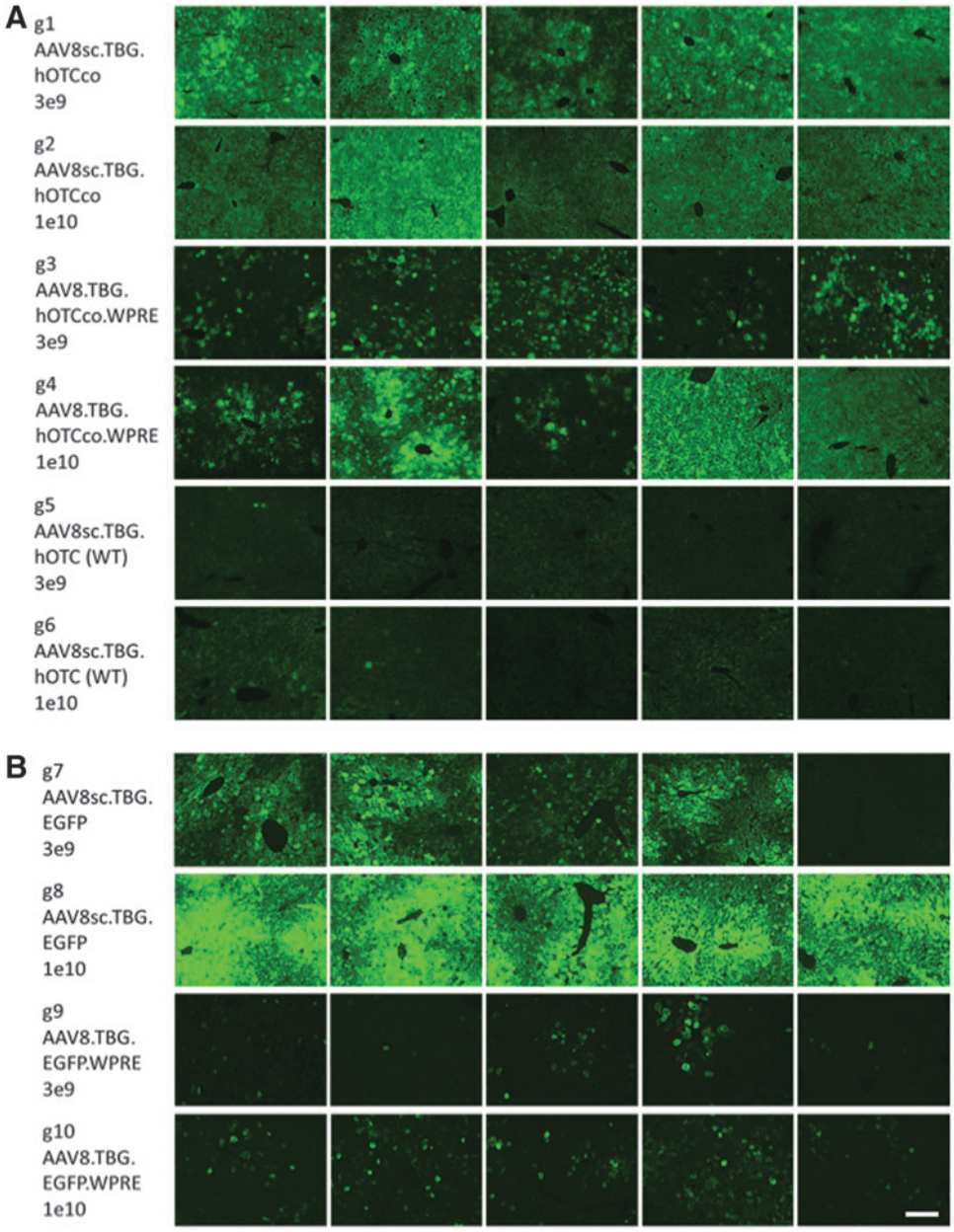

Figure 1. Representative images of liver sections from each animal showing human ornithine transcarbamylase (hOTC) or enhanced green fluorescent protein (EGFP) expression. (**A**) Detection of hOTC by immunofluorescence. (**B**) Detection of EGFP by direct fluorescence. Scale bar: 200 μm.

after vector administration. Liver sections were evaluated for hOTC expression by immunofluorescence and for EGFP expression by imaging direct EGFP fluorescence. Therefore, in both cases, the observed signal was green fluorescence (Fig. 1). Both the percentage of transgene expressing hepatocytes as well as measured overall fluorescence intensity were determined. As an additional control, EGFP and hOTC protein was also quantified by ELISA and immunoblot, respectively. To avoid the staining of endogenous mouse OTC protein, all experiments were performed in spf^{ash} mice, an animal model for OTC deficiency.[30,31] Due to abnormal splicing of OTC transcripts, this mouse model expresses only low (<10%) residual OTC activity in the liver, and immunostaining for OTC using the antibodies does not yield signals for endogenous OTC in these animals.[21,27]

Some variation of OTC expression levels was observed between animals within the same group. This variability can likely be ascribed to the fact that the spf^{ash} mouse is bred on a C3H× C57BL/6 background and shows some variation in

size, while dosing was not weight-based but on a per animal basis. Inconsistencies in injections seem less likely, but cannot be ruled out completely. Animals that received AAV8sc.TBG.EGFP at a dose of 1×10^{10} GC (Fig. 1B, g8) showed very low variation in EGFP expression levels, since they reached saturation of close to 100% of transduced liver area, whereas when EGFP expression was measured by intensity, g8 animals again showed variation in expression.

The difference between ss and sc vectors in hOTCco expression levels is dose dependent

For hOTCco-expressing vectors, the difference in expression levels based on area measurements between ss and sc vectors was found to be dose dependent (Fig. 2A). At the low dose of 3×10^{9} GC/animal, a more than sevenfold increase in the mean percentage of OTC-positive hepatocytes was observed with the sc version of the hOTCco-expressing vector compared with the ss version (Fig. 2A, group 1 [g1] vs. g3, $p\le0.01$). In contrast, at the higher dose of 1×10^{10}, merely a statistically insignificant ($p>0.05$) 1.24-fold increase in OTC-positive hepatocytes was achieved with the sc vector (Fig. 2A, g2 vs. g4).

A similar result was obtained when using hOTC immunofluorescence intensity as a measure of transduction (Fig. 3A). There was a 1.8-fold intensity difference between sc and ss vector at the 3×10^{9} dose (g1 vs, g3, $p\le0.0001$), but only a 1.1-fold difference at the 1×10^{10} dose (g2 vs. g4, $p>0.05$).

Interestingly, there was a small, statistically insignificant, inverse dose effect observed with the sc hOTCco vector, where the mean percentage of

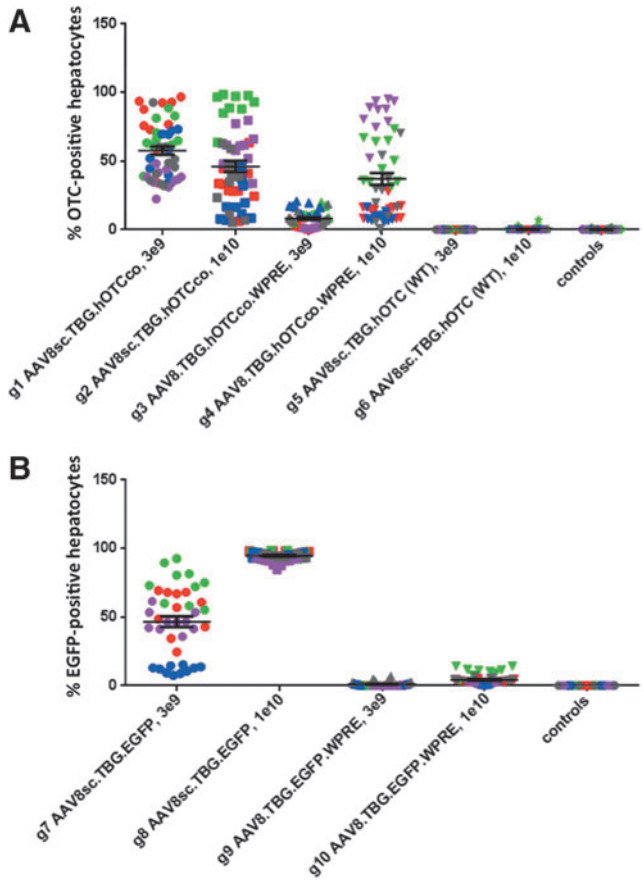

Figure 2. Analysis of hOTC and EGFP expression in the liver by transduced liver area. The expression levels of hOTC determined by immunostaining (**A**) and expression levels of EGFP determined by direct fluorescence (**B**) are shown from different vector constructs at two different doses (3×10^{9} and 1×10^{10} GC/mouse). Each data point shows the percentage of hOTC- or EGFP-positive liver area from one image; 10 images were taken for each animal. Data points from the same animal are shown using the identical color within each group. Bars show the mean percentage of transgene-positive liver area ± the standard error of the mean. Group numbers (**A**: g1–g6; **B**: g7–g10), type of vector, and dose are indicated.

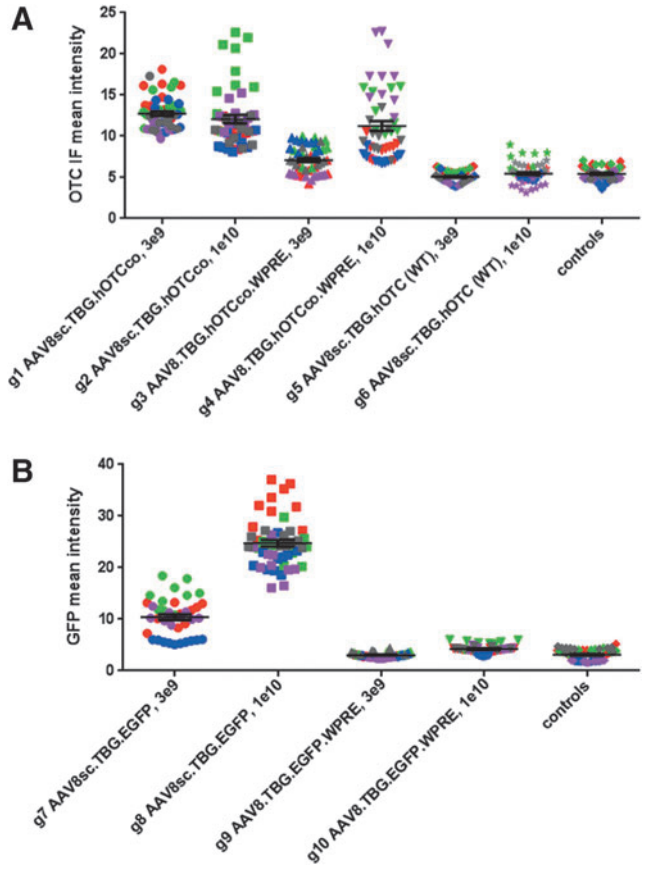

Figure 3. Analysis of hOTC and EGFP expression in liver by fluorescence intensity. Shown are the fluorescence intensities (mean gray values) from 10 liver images per animal for hOTC immunofluorescence (**A**) and EGFP direct fluorescence (**B**). Symbol and color of each data point is identical for the same animal, as in Fig. 2.

OTC-positive hepatocytes was 1.25-fold lower at the dose of 1×10^{10} versus 3×10^{9} (Fig. 2A, g1 vs. g2). A similar trend in transgene expression in hepatocytes has been observed in a previously published study using the same sc, codon-optimized hOTC vector.[21] As in the present study, the previous report showed a lower average level of OTC expression measured by immunofluorescence when using a dose of 1×10^{10} ($\sim$43%) compared with a dose of 3×10^{9} ($\sim$57%). Since the high-dose sc vector in this study achieved only about 46% of positive hepatocytes, it appears unlikely that the lack of increase in expression levels with the sc vector represents an artifact due to saturation effects.

To corroborate the results obtained by image analysis (*i.e.*, percent of transgene positive area and immunofluorescence intensity), Western blotting was performed on liver lysates, and the intensity of fluorescent bands normalized to cyclophilin A was analyzed (Fig. 4A). With this analysis, the expression level of sc hOTCco did follow a dose response and was higher at the dose of 1×10^{10} compared with 3×10^{9}. However, as observed before, the difference between ss and sc hOTCco vector was again higher at the low dose (7.9-fold difference between g1 and g3) as it was at the high dose (2.0-fold difference between g2 and g4; Fig. 4A).

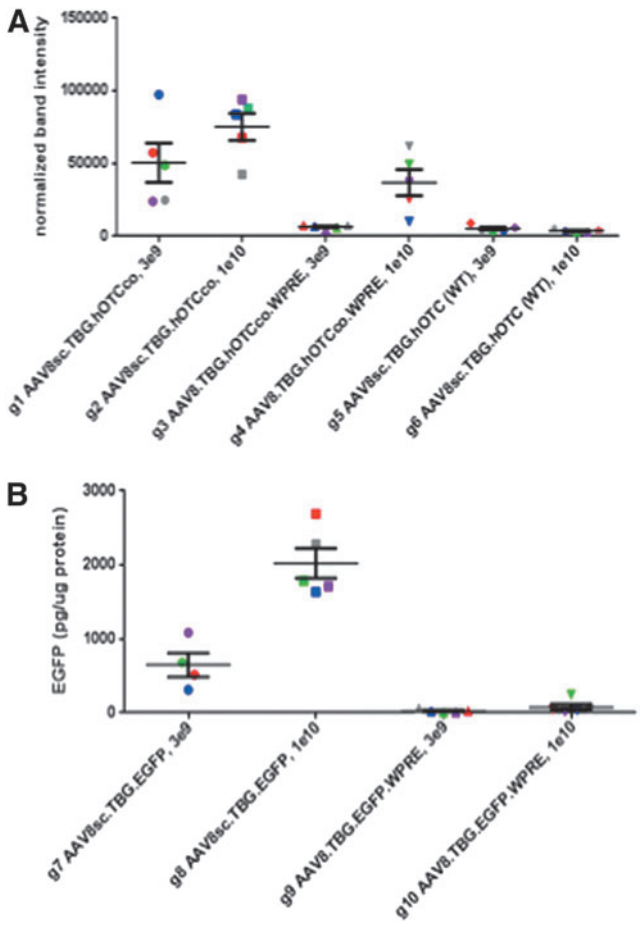

Figure 4. Analysis of hOTC and EGFP expression levels by Western blot and enzyme-linked immunosorbent assay (ELISA). Liver protein levels samples for hOTC determined by Western blotting (**A**) and for EGFP by ELISA (**B**) are shown. Bands from Western blots were quantified with fluorescent antibodies using a Licor Odyssey instrument and normalized for cyclophilin A as reference protein. Each data point represents one animal with identical symbol and color for each animal, as in Fig. 2.

The difference between ss and sc vectors at the high dose is transgene specific

At the low dose of 3×10^{9}, both the codon-optimized *hOTC* vector and the *EGFP*-expressing vector showed similar increases in expression levels when the sc modification was incorporated (Fig. 2A, g1 vs. g3, $p\le0.01$; Fig. 2B, g7 vs. g9, $p\le0.01$; mean differences in percent positive hepatocytes of 50% for hOTCco and 46% for EGFP). However, this was not the case at the higher vector dose of 1×10^{10}, where only the *EGFP* vector gained improvement with the sc version. Here, while 1×10^{10} of *hOTC*co-expressing vector showed only a minimal (1.2-fold) increase in positive hepatocytes when transitioning from the ss to sc version (Fig. 2A, g2 vs. g4, $p>0.05$), the change from ss to sc vector yielded a substantial (22.4-fold) increase in the mean percentage of transgene-positive hepatocytes at this dose when *EGFP* was the transgene (Fig. 2B, g8 vs. g10, $p\le0.0001$). This finding was due in part to the fact that the ss *EGFP* vector yielded only minimal expression levels at 1×10^{10} GC/mouse (Fig. 2B, g10, mean positive area 4%), which was in stark contrast to the ss *hOTC*co vector with a mean positive area of 37% (Fig. 2A, g4). Moreover, the sc *EGFP* vector plateaued at high mean levels of positive area near 100% (Fig. 2B, g8, 95%), whereas the sc *hOTC*co vector reached a mean of only 46% (Fig. 2A, g2). In other words, with an *EGFP* transgene, the advantage of using sc vectors was independent of the dose, whereas the use of sc vectors expressing *hOTC*co was only beneficial in increasing expression at the lower dose of 3×10^{9}.

These findings, based on measurements of transgene-positive area, were again confirmed when analyzing EGFP and hOTC image intensities (Fig. 3). With co *hOTC* as transgene, there was a 1.8-fold increase in mean fluorescence intensity of immunostains at the 3×10^{9} dose (g1 vs. g3, $p\le0.0001$), but merely a 1.1-fold increase at the 1×10^{10} dose (g2 vs. g4, $p>0.05$) when using the

codon-optimized vector instead of the ss version (Fig. 3A). In contrast, using *EGFP* as transgene, considerable increases in mean fluorescence intensity could be measured by using the sc vector version both at the low dose of 3×10^9 (3.4-fold increase; g7 vs. g9, $p\le0.0001$) and at the high dose of 1×10^{10} (5.8-fold increase; g8 vs. g10, $p\le0.0001$; Fig. 3B).

Protein data by ELISA for EGFP and Western blot for hOTC corroborate the finding that the difference between ss and sc vectors at the high dose of 1×10^{10} is high with *EGFP* as transgene (27.5-fold difference between g8 and g10; Fig. 4B), but only moderate when *hOTC* is the transgene (2.0-fold difference between g2 and g4; Fig. 4A).

A previous publication by Wu *et al*. employed *in situ* hybridization and immunohistochemistry to compare the hepatic expression pattern of ss AAV2.hFIX with that of the sc version of the vector at high doses (3×10^{10}–10×10^{10} GC/animal) in mice expressing equivalent circulating FIX.[13] In their study, the ss vector resulted in transduction of few hepatocytes showing strong hFIX expression, whereas the sc vector yielded widespread transduction with lower expression levels on a per cell basis. These findings with hFIX are similar to the present results with hOTCco and EGFP, where few hepatocytes with a strong fluorescence signal after administration of the ss vectors and widespread expression patterns with the sc vectors were also observed. However, in the present study, sc vector delivery resulted in a mixture of hepatocytes with both weak and strong fluorescence (Fig. 1).

It is important to note that the ss vectors (for both *EGFP* and *hOTC*co) carried a WPRE element that was absent in the sc versions of the vectors due to size restrictions. The WPRE element has been shown to enhance mRNA stability and thus increase expression levels.[32–34] Therefore, the presence of this element could have given the ss vectors an advantage over the sc versions in terms of increased expression. Even if this was the case, however, the WPRE element did not overcome the increase in expression levels gained through self-complementarity. In fact, all ss vectors with the WPRE element showed virtually no or very low expression levels, with the exception of the high-dose *hOTC*co vector that achieved 37% positive area (Fig. 2A, g4). Although not statistically significant, this was still lower than the expression level achieved by its sc counterpart without the WPRE element (Fig. 2A, g2, 46% positive area).

Codon optimization is more effective in increasing expression levels than the use of sc vectors

In addition to the use of self-complementarity to improve transgene expression, the relative impact of codon optimization was also of interest. Note that the effect of codon optimization could not be tested for the *EGFP* vectors, as this transgene already contains an optimized sequence. However, it was possible to compare both co and WT (non-codon-optimized) versions of the *hOTC* vector in the model. Overall, the findings indicated that while the use of sc instead of ss vectors showed strong improvements in expression levels (with the exception of *hOTC*co at 1×10^{10} GC/mouse), the use of codon-optimized vectors allowed even greater increases in expression when compared with vectors containing an unaltered nucleotide sequence. The sc vector carrying the non-codon-optimized *hOTC* transgene failed to yield any appreciable expression levels at either the low or high dose, with no statistically significant difference between the two dosing groups (Fig. 2A, g5 and g6). In comparison, using the codon-optimized version of this sc vector changed expression levels dramatically, reaching mean percentages of positive liver area of 58% at the 3×10^9 dose and 46% at the 1×10^{10} dose (Fig. 2A, g1 and g2, respectively).

A nearly identical observation was made when measuring the mean fluorescence intensity for hOTC immunostaining (Fig. 3A). Expression from the non-codon-optimized vectors remained near background levels at doses of both 3×10^9 (g5, mean intensity 5.1) and 1×10^{10} (g6, mean intensity 5.5), whereas the codon-optimized versions of the vector achieved fluorescence intensity levels of 12.8 (g1, 3×10^9 dose) and 12.1 (g2, 1×10^{10} dose).

The stronger increases in hOTC expression levels when using co vectors compared to sc vectors were further confirmed by Western blot data, showing again extremely low hOTC levels with non-codon-optimized vectors (g5 and g6; Fig 4A), but high expression when co vectors had been utilized (g1 and g2; Fig 4A).

Codon optimization has frequently been used to enhance expression of secreted proteins from viral vectors, which can be measured in samples obtained from blood. For instance, codon optimization of a human factor VII transgene yielded a 37-fold increase in expression when delivered to mice in a sc AAV8 vector.[12] In addition, the expression of codon-optimized human factor VIII constructs also reached a 29- to 44-fold increase when delivered to mice via lentiviral vectors.[11] In the study by Wu *et al.*, the impact of both codon optimization

and self-complementarity were compared for an AAV2.hFIX vector at a dose range of 3×10^{9} to 1×10^{11} GC/mouse. Similar to the present study, the authors found that while a 1.5- to 2.6-fold increase in expression levels occurred when comparing an sc vector with the ss version (both non-codon-optimized), a more substantial 5.5- to 21.2-fold increase was observed when the codon-optimized sc vector was used instead of the non-codon-optimized ss version.[13]

The *hOTC* gene is potentially more amenable to gains in expression by codon-optimization than most other genes because the *OTC* sequence contains a particularly high number of rare codons (GenScript Rare Codon Analysis Tool). It is therefore possible that by codon-optimizing *hOTC* a higher level of improvement in expression was achieved than what would be possible in genes that contain fewer rare codons.

Correlation between number of vector genomes in liver and expression levels

This study went on to analyze liver tissue from all treated animals in order to determine the average number of vector genomes for each of the constructs (expressed as GCs per diploid mouse genome; *i.e.*, per cell if ignoring that some hepatocytes contain more than one nucleus). In general, at each vector dose, higher vector DNA copy numbers were achieved by the sc vectors when compared with their ss counterparts for both the *EGFP* and *hOTC*co transgenes (Fig. 5). A potential explanation could be that the sc vectors are more stable and persistent in the transduced cells.

For the *EGFP*-expressing vectors, a correlation was observed between the number of vector genomes in liver and transgene-expressing hepatocytes. With the increasing presence of vector DNA, the percentage of GFP-positive liver area increased until reaching a plateau between 90% and 100% positive area (Fig. 5B). This was not the case for vectors expressing the *hOTC* transgene (Fig. 5A). At the dose of 1×10^{10} GC/mouse, OTC-positive hepatocytes were much lower than expected, given the high number of vector genomes present in liver for all three vector types (sc *hOTC*co, ss *hOTC*co, and sc *hOTC* [WT]). For the high dose sc *hOTC*co vector, there even appeared to be an inverse correlation between number of vector genomes and OTC-positive hepatocytes. Potential reasons for this behavior could include toxicity due to overexpression of the hOTC protein. At the lower dose of 3×10^{9}, the weak correlation between GCs and OTC-positive hepatocytes was only observed in the non-codon-optimized sc *hOTC* (WT) vector, which

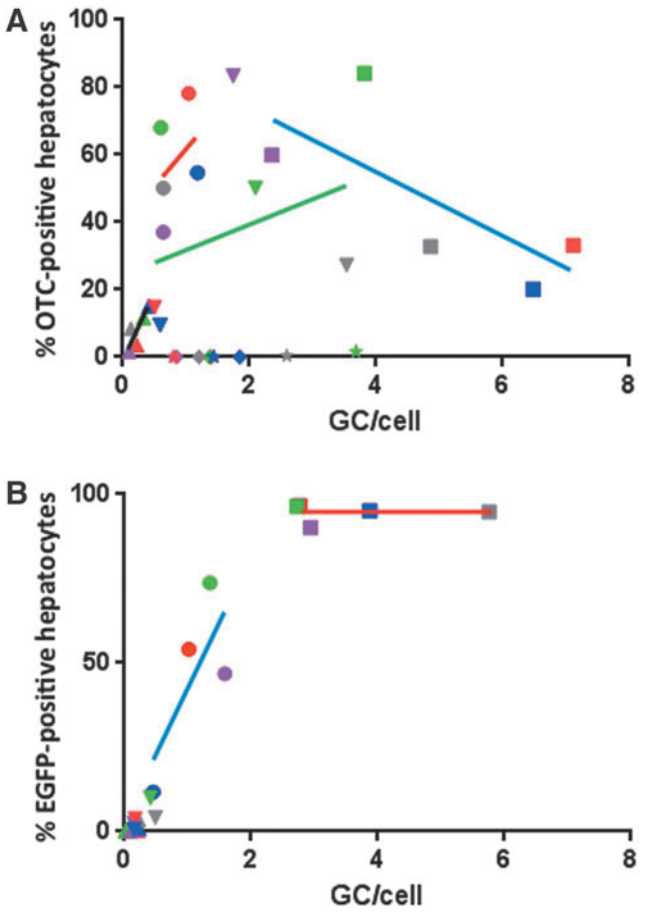

Figure 5. Expression levels plotted against vector genome copies in liver. For hOTC (**A**) and EGFP (**B**), each data point represents a single animal, and expression levels are the average percentage of transgene-positive liver area from 10 images/animal. Shape and color of each symbol are identical for individual animals as in previous figures. For some groups, linear regression lines were drawn with Graphpad Prism. (**A**) (hOTC): circle, g1 (AAV8sc.TBG.hOTCco, 3e9); square, g2 (AAV8sc.TBG.hOTCco, 1e10); triangle, g3 (AAV8.TBG.hOTCco.WPRE, 3e9); inverted triangle, g4 (AAV8.TBG.hOTCco.WPRE, 1e10); diamond, g5 (AAV8sc.TBG.hOTC [WT], 3e9); star, g6 (g6 AAV8sc.TBG.hOTC [WT], 1e10). Line colors are red for g1, blue for g2, black for g3, and green for g4. (**B**) (EGFP): circle, g7 (AAV8sc.TBG.EGFP, 3e9); square, g8 (AAV8sc.TBG.EGFP, 1e10); triangle, g9 (AAV8.TBG.EGFP.WPRE, 3e9); inverted triangle, g10 (AAV8.TBG.EGFP.WPRE, 1e10). Line colors are blue for g7 and red for g8.

yielded relatively high copy numbers in liver but little to no transgene expression (Fig. 5A, g5). The presence of non-codon-optimized vector genomes in hepatocytes without detectable hOTC expression suggests that translation is inefficient in these cells. More similar to what was observed with *EGFP*, the codon-optimized versions of sc and ss *hOTC* demonstrated a more direct correlation between increasing expression levels and increasing presence of vector genomes when injected at the lower dose (Fig. 5A, g1 and g3). In other words, codon optimization increased the number of posi-

tive hepatocytes detectable by histological analysis, rather than leaving the number of positive hepatocytes constant and merely increasing the level of visible protein within those cells.

Overall, the goal of this study was to determine the impact of vector modifications on the expression of non-secreted reporter or therapeutic proteins. The findings indicate that while the conversion of ss to sc vectors can improve transgene expression levels, this effect can be influenced by both transgene and dose. Where the improvement of expression levels when using ss instead sc *EGFP*-containing vectors proved dose-independent, the impact of self-complementarity for *hOTC*co-containing vectors was dose-dependent. Furthermore, compared with the addition of self-complementarity on a codon-optimized AAV8.hOTC backbone, the addition of codon optimization on a sc AAV8.hOTC backbone demonstrated a greater impact on improved transgene expression. These findings indicate the importance of continued efforts in optimizing AAV vector modification schemes, as well as the need for investigating the effects of these modifications on a given transgene and dosing platform when developing AAV-based gene therapy approaches for a specific disease model.

ACKNOWLEDGMENTS

We thank the Vector and Animal Models Cores of the Gene Therapy Program for their support. This work was supported by a grant from Dimension Therapeutics.

AUTHOR DISCLOSURE

J.M.W is an advisor to REGENXBIO, Dimension Therapeutics, Solid Gene Therapy, and is a founder of, holds equity in, and has a sponsored research agreement with REGENXBIO and Dimension Therapeutics; in addition, he is a consultant to several biopharmaceutical companies and is an inventor on patents licensed to various biopharmaceutical companies. No competing financial interests exist for the remaining authors.

REFERENCES

1. Ferrari FK, Samulski T, Shenk T, et al. Second-strand synthesis is a rate-limiting step for efficient transduction by recombinant adeno-associated virus vectors. J Virol 1996;70:3227–3234.
2. Fisher KJ, Gao GP, Weitzman MD, et al. Transduction with recombinant adeno-associated virus for gene therapy is limited by leading-strand synthesis. J Virol 1996;70:520–532.
3. McCarty DM. Self-complementary AAV vectors; advances and applications. Mol Ther 2008;16: 1648–1656.
4. Nakai H, Storm TA, Kay MA. Recruitment of single-stranded recombinant adeno-associated virus vector genomes and intermolecular recombination are responsible for stable transduction of liver *in vivo*. J Virol 2000;74:9451–9463.
5. McCarty DM, Fu H, Monahan PE, et al. Adeno-associated virus terminal repeat (TR) mutant generates self-complementary vectors to overcome the rate-limiting step to transduction *in vivo*. Gene Ther 2003;10:2112–2118.
6. Wang Z, Ma HI, Li J, et al. Rapid and highly efficient transduction by double-stranded adeno-associated virus vectors *in vitro* and *in vivo*. Gene Ther 2003;10:2105–2111.
7. Fagone P, Wright JF, Nathwani AC, et al. Systemic errors in quantitative polymerase chain reaction titration of self-complementary adeno-associated viral vectors and improved alternative methods. Hum Gene Ther Methods 2012;23:1–7.
8. Mauro VP, Chappell SA. A critical analysis of codon optimization in human therapeutics. Trends Mol Med 2014;20:604–613.
9. Angov E. Codon usage: nature's roadmap to expression and folding of proteins. Biotechnol J 2011;6:650–659.
10. Plotkin JB, Kudla G. Synonymous but not the same: the causes and consequences of codon bias. Nat Rev Genet 2011;12:32–42.
11. Ward NJ, Buckley SM, Waddington SN, et al. Codon optimization of human factor VIII cDNAs leads to high-level expression. Blood 2011;117: 798–807.
12. Binny C, McIntosh J, Della Peruta M, et al. AAV-mediated gene transfer in the perinatal period results in expression of FVII at levels that protect against fatal spontaneous hemorrhage. Blood 2012; 119:957–966.
13. Wu Z, Sun J, Zhang T, et al. Optimization of self-complementary AAV vectors for liver-directed expression results in sustained correction of hemophilia B at low vector dose. Mol Ther 2008;16: 280–289.
14. Nathwani AC, Gray JT, Ng CY, et al. Self-complementary adeno-associated virus vectors containing a novel liver-specific human factor IX expression cassette enable highly efficient transduction of murine and nonhuman primate liver. Blood 2006;107:2653–2661.
15. Hinderer C, Bell P, Gurda BL, et al. Intrathecal gene therapy corrects CNS pathology in a feline model of mucopolysaccharidosis I. Mol Ther 2014; 22:2018–2027.
16. Hinderer C, Bell P, Gurda BL, et al. Liver-directed gene therapy corrects cardiovascular lesions in feline mucopolysaccharidosis type I. Proc Natl Acad Sci U S A 2014;111:14894–14899.
17. Hinderer C, Bell P, Louboutin JP, et al. Neonatal systemic AAV induces tolerance to CNS gene therapy in MPS I dogs and nonhuman primates. Mol Ther 2015;23:1298–1307.
18. Sack BK, Merchant S, Markusic DM, et al. Transient B cell depletion or improved transgene expression by codon optimization promote tolerance to factor VIII in gene therapy. PloS One 2012; 7:e37671.
19. Foster H, Sharp PS, Athanasopoulos T, et al. Codon and mRNA sequence optimization of microdystrophin transgenes improves expression and physiological outcome in dystrophic mdx mice following AAV2/8 gene transfer. Mol Ther 2008; 16:1825–1832.
20. Dominguez E, Marais T, Chatauret N, et al. Intravenous scAAV9 delivery of a codon-optimized SMN1 sequence rescues SMA mice. Hum Mol Genet 2011;20:681–693.
21. Wang L, Morizono H, Lin J, et al. Preclinical evaluation of a clinical candidate AAV8 vector for ornithine transcarbamylase (OTC) deficiency

reveals functional enzyme from each persisting vector genome. Mol Genet Metab 2012;105:203–211.

22. Nathwani AC, Reiss UM, Tuddenham EG, et al. Long-term safety and efficacy of factor IX gene therapy in hemophilia B. New Engl J Med 2014; 371:1994–2004.

23. Nathwani AC, Tuddenham EG, Rangarajan S, et al. Adenovirus-associated virus vector-mediated gene transfer in hemophilia B. New Engl J Med 2011; 365:2357–2365.

24. Gao G, Lu Y, Calcedo R, et al. Biology of AAV serotype vectors in liver-directed gene transfer to nonhuman primates. Mol Ther 2006;13: 77–87.

25. Lock M, Alvira M, Vandenberghe LH, et al. Rapid, simple, and versatile manufacturing of recombinant adeno-associated viral vectors at scale. Hum Gene Ther 2010;21:1259–1271.

26. Lock M, Alvira MR, Chen SJ, et al. Absolute determination of single-stranded and self-complementary adeno-associated viral vector genome titers by droplet digital PCR. Hum Gene Ther Methods 2014;25:115–125.

27. Wang L, Wang H, Morizono H, et al. Sustained correction of OTC deficiency in spf(ash) mice using optimized self-complementary AAV2/8 vectors. Gene Ther 2012;19:404–410.

28. Bell P, Moscioni AD, McCarter RJ, et al. Analysis of tumors arising in male B6C3F1 mice with and without AAV vector delivery to liver. Mol Ther 2006;14:34–44.

29. Wang L, Calcedo R, Bell P, et al. Impact of preexisting immunity on gene transfer to nonhuman primate liver with adeno-associated virus 8 vectors. Hum Gene Ther 2011;22:1389–1401.

30. Rosenberg LE, Kalousek F, Orsulak MD. Biogenesis of ornithine transcarbamylase in spfash mutant mice: two cytoplasmic precursors, one mitochondrial enzyme. Science 1983;222:426–428.

31. Hodges PE, Rosenberg LE. The spfash mouse: a missense mutation in the ornithine transcarbamylase gene also causes aberrant mRNA splicing. Proc Natl Acad Sci U S A 1989;86:4142–4146.

32. Loeb JE, Cordier WS, Harris ME, et al. Enhanced expression of transgenes from adeno-associated virus vectors with the woodchuck hepatitis virus posttranscriptional regulatory element: implications for gene therapy. Hum Gene Ther 1999;10: 2295–2305.

33. Paterna JC, Moccetti T, Mura A, et al. Influence of promoter and WHV post-transcriptional regulatory element on AAV-mediated transgene expression in the rat brain. Gene Ther 2000;7:1304–1311.

34. Mian A, McCormack WM Jr, Mane V, et al. Long-term correction of ornithine transcarbamylase deficiency by WPRE-mediated overexpression using a helper-dependent adenovirus. Mol Ther 2004;10:492–499.

Received for publication March 25, 2016;
accepted after revision November 22, 2016.

Published online: November 30, 2016.